

Supplementary information for:

“Avoiding problem reactions at the ferrocenyl-alkyne motif: a convenient synthesis of model, redox-active complexes for molecular electronics”

Michael S. Inkpen, Andrew J. P. White, Tim Albrecht,* Nicholas J. Long*

Department of Chemistry, Imperial College London, London SW7 2AZ, U.K.; Tel: +44 (0)20 7594 5781;

E-mail: n.long@imperial.ac.uk; t.albrecht@imperial.ac.uk

CONTENTS

S1: EXPERIMENTAL

S7: REACTION SCHEMES

S9: $^1\text{H}/^{13}\text{C}\{^1\text{H}\}$ NMR AND MASS SPECTRA

S20: ELECTROCHEMISTRY

S23: X-RAY CRYSTALLOGRAPHY

S25: REFERENCES

EXPERIMENTAL

All preparations were carried out using standard Schlenk line and air-sensitive chemistry techniques under an atmosphere of nitrogen. No special precautions were taken to exclude air or moisture during workup, unless otherwise stated. Solvents used in reactions were sparged with nitrogen and dried with alumina beads, Q5 Copper catalyst on molecular sieves, or 3A molecular sieves,¹ where appropriate. Organic solvents used in electrochemical experiments were of HPLC grade (HiPerSolv CHROMANORM, VWR), and water was purified using a Purite Select Fusion system to a resistivity of 15-18.2 M Ω .cm. Neutral alumina of Brockmann activity V (15% H₂O) and silica were used for chromatographic separations. 1,1'-Diiodoferrocene,² 2-(trimethylsilyl)ethyl-4'-ethynylphenyl sulfide (Scheme S-1),³ $\text{fcI}(\text{C}\equiv\text{C}-m\text{-Py})^4$ and $(\mu\text{-}3,5\text{-Py})(\text{C}\equiv\text{C}-[\text{fc}]\text{-I})_2^4$ were prepared via literature methods from commercially available starting materials. 1,1'-Bis(phenylethynyl)ferrocene was obtained from a crude sample⁵ following pre-

absorption on silica, purification by column chromatography (silica; *n*-hexane→CH₂Cl₂/*n*-hexane [1:4]) and recrystallization from CH₂Cl₂/*n*-hexane. Gold and platinum wire used for electrodes was obtained from Goodfellow (1 mm diameter, >99.9% purity).

¹H and ¹³C{¹H} NMR spectra were recorded at ambient temperature on a Bruker 400 MHz spectrometer and internally referenced to the residual solvent peaks of CDCl₃ at δ 7.26 (¹H) and 77.16 ppm (¹³C{¹H}).⁶ ¹³C{¹H} spectra were fully assigned where possible using 2D correlation spectroscopy. IR spectra were recorded on a PerkinElmer Spectrum 100 FT-IR spectrometer. Mass spectrometry analyses were conducted by the Mass Spectrometry Service, Imperial College London. Microanalyses were carried out by Stephen Boyer of the Science Centre, London Metropolitan University.

Electrochemical experiments were conducted under an atmosphere of argon. Potentials are reported relative to [FeCp₂]⁺/[FeCp₂], measured against an internal [FeCp₂]⁺/[FeCp₂] or [FeCp*₂]⁺/[FeCp*₂] reference, where appropriate. Solution electrochemical studies were performed in CH₂Cl₂/0.1 M ⁿBu₄NPF₆ or CH₂Cl₂/~0.02 M Na[B(C₆H₃(CF₃)₂)₄] on a CHI760C potentiostat (CH Instruments, Austin, Texas) with a glassy carbon disc as working electrode (diameter = 5 mm), and Pt-wire reference and counter electrodes. Analyte solutions were between 0.1-1 mM. Surface electrochemical studies were performed in H₂O/0.1 M HClO₄ or CH₃CN/0.1 M ⁿBu₄NPF₆ on a Reference 600 potentiostat (Gamry Instruments, Warminster, Pennsylvania) with Ag/AgCl or Pt-wire (pseudo) reference electrode (CH Instruments, Austin, Texas), Pt-wire counter electrodes and a surface-modified gold bead (**1c-Au**) as working electrode. The latter was positioned in the solution such that the bead was immersed just below the surface of the electrolyte, taking care that as little of the connecting wire as possible was exposed to the solution. Electrical connection was made to the other end of the wire. The gold bead electrodes (Ø = 0.2-0.3 mm) were prepared by melting one end of a 1 mm gold wire into a spherical ball using a hydrogen-oxygen flame. Prior to use, these were flame-annealed, immersed into aliquots of coating solution (~1 mM in **1b/1c**) for ~20 h at room temperature, rinsed with ethanol and dried in a stream of nitrogen. Coating solutions ~1 mM in **1c** were prepared by stirring a mixture of **1a** (0.007 g, 0.01 mmol), THF (5 mL) and 1.0 M tetra-*n*-butylammonium fluoride in THF (5 mL, 5 mmol) for 1 h at 37°C.⁷ After cooling, solutions were decanted and stored at -20°C in capped polypropylene vials until use. These appeared reasonably

stable in air, facilitating the production of surface-modified gold bead electrodes with reproducible electrochemistry for at least 1 month.

fc(C≡C-*p*-C₆H₄-S-CH₂CH₂-SiMe₃)₂ (1a**)**

A solution of THF (3 mL), 1,1'-diiodoferrocene (0.303 g, 0.69 mmol) and 2-(trimethylsilyl)ethyl-4'-ethynylphenyl sulfide (**L**) (0.351 g, 1.50 mmol) was sparged with nitrogen for ~15 min. Pd(P^{*t*}Bu₃)₂ (0.023 g, 0.04 mmol), CuI (0.010 g, 0.05 mmol) and diisopropylamine (1 mL) were added, and the resulting mixture stirred for 18 h. After removal of solvent the crude material was preabsorbed onto silica and purified by column chromatography, packing with *n*-hexane and eluting with CH₂Cl₂/*n*-hexane (1:4 v/v). Orange-red fractions were collected, dried *in vacuo* and recrystallized from CH₂Cl₂/*n*-hexane to provide red crystals of **1a** (0.348 g, 77%). Crystals suitable for X-ray diffraction were obtained by slow evaporation of an *n*-hexane solution. ¹H NMR (400 MHz, CDCl₃): δ (ppm) 0.06 (s, 18H, Si-CH₃), 0.94 (m, 4H, CH₂), 2.97 (m, 4H, CH₂), 4.31 (pseudo-t, *J*_{αβ} = 1.9 Hz, 4H, Cp-H), 4.53 (pseudo-t, *J*_{αβ} = 1.9 Hz, 4H, Cp-H), 7.16 (d, *J* = 8.3 Hz, 4H, Ar-H), 7.32 (d, *J* = 8.4 Hz, 4H, Ar-H). ¹³C{¹H} NMR (100 MHz, CDCl₃): δ (ppm) 1.69 (Si-CH₃), 16.70 (CH₂), 29.07 (CH₂), 67.16 (Cp, C-C≡C), 70.93 (Cp, C-H), 72.94 (Cp, C-H), 86.46 (C≡C), 87.43 (C≡C), 120.70 (Ar, C-C≡C), 127.91 (Ar, C-H), 131.70 (Ar, C-H), 137.46 (Ar, C-S). IR (ATR): ν (cm⁻¹) 2207w (C≡C). HR-MS ES⁺: *m/z* 650.1648 ([M]⁺ Calc.: 650.1616). (Found: C, 66.42; H, 6.47. Calc. for C₃₆H₄₂FeS₂Si₂: C, 66.43; H, 6.50%).

fc(C≡C-*p*-C₆H₄-S-Me)₂ (1b**)**

A mixture of **1a** (0.102 g, 0.16 mmol) and 1.0 M tetra-*n*-butylammonium fluoride in THF (12.5 mL, 12.5 mmol) was stirred at room temperature for 1 h, at which point methyl iodide (3.75 mL, 60.24 mmol) was added. After a further 20 min, the solution was diluted into CH₂Cl₂ (120 mL) and H₂O (20 mL), whereby the organic fraction was isolated, dried over NaSO₄ and filtered through Celite. The filtrate was concentrated and then loaded onto a silica column packed with *n*-hexane. Elution with CH₂Cl₂/*n*-hexane (6:4 v/v) developed an orange band which was collected, dried *in vacuo* and recrystallized by evaporation of an *n*-pentane solution to provide red crystals

of **1b** (0.058 g, 77%). ¹H NMR (400 MHz, CDCl₃): δ (ppm) 2.49 (s, 6H, S-CH₃), 4.31 (pseudo-t, *J*_{αβ} = 1.8 Hz, 4H, Cp-H), 4.53 (pseudo-t, *J*_{αβ} = 1.9 Hz, 4H, Cp-H), 7.09 (d, *J* = 8.5 Hz, 4H, Ar-H), 7.29 (d, *J* = 8.5 Hz, 4H, Ar-H). ¹³C{¹H} NMR (100 MHz, CDCl₃): δ (ppm) 15.60 (S-CH₃), 67.53 (Cp, C-C≡C), 70.86 (Cp, C-H), 72.96 (Cp, C-H), 86.68 (C≡C), 87.21 (C≡C), 120.28 (Ar, C-C≡C), 125.93 (Ar, C-H), 131.79 (Ar, C-H), 138.51 (Ar, C-S). IR (ATR): ν (cm⁻¹) 2205w (C≡C). HR-MS ES⁺: *m/z* 478.0506 ([M]⁺ Calc.: 478.0512). (Found: C, 70.14; H, 4.76. Calc. for C₂₈H₂₂FeS₂: C, 70.29; H, 4.63%).

fc(C≡C-*m*-Py)(C≡C-*p*-C₆H₄-S-CH₂CH₂-SiMe₃) (2)

A solution of THF (3 mL), diisopropylamine (1 mL), fcI(C≡C-*m*-Py) (0.200 g, 0.48 mmol) and 2-(trimethylsilyl)ethyl-4'-ethynylphenyl sulfide (**L**) (0.126 g, 0.54 mmol) was sparged with nitrogen for ~5 min. Pd(P^tBu₃)₂ (0.008 g, 0.02 mmol) and CuI (0.003 g, 0.02 mmol) were added and the resulting mixture stirred for 20 h. After removal of solvent the crude material was purified by column chromatography (silica; CH₂Cl₂). The second orange-red band was isolated, dried *in vacuo* and recrystallized from CH₂Cl₂/*n*-hexane to provide orange-red crystals of **1a** (0.149 g, 59%). ¹H NMR (400 MHz, CDCl₃): δ (ppm) 0.05 (s, 9H, Si-CH₃), 0.93 (m, 2H, CH₂), 2.96 (m, 2H, CH₂), 4.31 (pseudo-t, *J*_{αβ} = 1.6 Hz, 2H, Cp-H), 4.34 (pseudo-t, *J*_{αβ} = 1.7 Hz, 2H, Cp-H), 4.54 (pseudo-t, *J*_{αβ} = 1.7 Hz, 2H, Cp-H), 4.56 (pseudo-t, *J*_{αβ} = 1.7 Hz, 2H, Cp-H), 7.13 (m, 3H, Ar-H and Py-H_m), 7.29 (d, 2H, *J* = 8.3 Hz, Ar-H), 7.61 (dt, 1H, Py-H_p), 8.48 (br s, 1H, Py-H_o), 8.66 (br s, 1H, Py-H_o). ¹³C{¹H} NMR (100 MHz, CDCl₃): δ (ppm) -1.62 (Si-CH₃), 16.79 (CH₂), 29.19 (CH₂), 66.44 (Cp, C-C≡C), 67.63 (Cp, C-C≡C), 70.91 (Cp, C-H), 71.15 (Cp, C-H), 73.02 (Cp, C-H), 73.14 (Cp, C-H), 83.51 (C≡C), 86.80 (C≡C), 87.19 (C≡C), 90.95 (C≡C), 120.67 (Ar, C-C≡C), 121.14 (Py, C-C≡C), 123.01 (Py, C-H_m), 128.01 (Ar, C-H), 131.69 (Ar, C-H), 137.58 (Ar, C-S), 138.16 (Py, C-H_p), 147.93 (Py, C-H_o), 152.14 (Py, C-H_o). IR (ATR): ν (cm⁻¹) 2212 (C≡C). HR-MS ES⁺: *m/z* 520.1199 ([M+H]⁺ Calc.: 520.1218). (Found: C, 69.35; H, 5.63; N, 2.70. Calc. for C₃₀H₂₉FeNSSi: C, 69.20; H, 5.46; N, 2.63%).

(μ-3,5-Py)(C≡C-[fc]-C≡C-*p*-C₆H₄-S-CH₂CH₂-SiMe₃)₂ (3)

A solution of THF (3 mL), diisopropylamine (1 mL), (μ-3,5-Py)(C≡C-[fc]-I)₂ (0.199 g, 0.27 mmol) and 2-(trimethylsilyl)ethyl-4'-ethynylphenyl sulfide (**L**) (0.143 g, 0.61 mmol) was sparged with nitrogen for ~5 min. Pd(P^tBu₃)₂ (0.009 g, 0.02 mmol) and CuI (0.003 g, 0.02 mmol)

were added and the resulting mixture stirred for 20 h. After removal of solvent the crude material was purified by column chromatography on alumina grade V, packing with *n*-hexane and eluting with CH₂Cl₂/*n*-hexane (3:7 v/v). Fractions containing the product were combined and reduced in volume through solvent evaporation, precipitating a bright orange solid. This was filtered, washed with *n*-hexane, and dried *in vacuo* to provide **3** (0.178 g, 70%). ¹H NMR (400 MHz, CDCl₃): δ (ppm) 0.04 (s, 18H, Si-CH₃), 0.92 (m, 4H, CH₂), 2.94 (m, 4H, CH₂), 4.33 (pseudo-t, *J*_{αβ} = 1.6 Hz, 4H, Cp-H), 4.36 (pseudo-t, *J*_{αβ} = 1.6 Hz, 4H, Cp-H), 4.55 (pseudo-t, *J*_{αβ} = 1.7 Hz, 4H, Cp-H), 4.57 (pseudo-t, *J*_{αβ} = 1.7 Hz, 4H, Cp-H), 7.15 (d, *J* = 8.3, Ar-H), 7.30 (d, *J* = 8.3, Ar-H), 7.66 (t, *J* = 1.9, Py-H_p), 8.48 (d, *J* = 1.9, Py-H_o). ¹³C{¹H} NMR (100 MHz, CDCl₃): δ (ppm) -1.58 (Si-CH₃), 16.81 (CH₂), 29.19 (CH₂), 66.18 (Cp, C-C≡C), 67.65 (Cp, C-C≡C), 71.06 (Cp, C-H), 71.36 (Cp, C-H), 73.06 (Cp, C-H), 73.23 (Cp, C-H), 82.95 (C≡C), 86.88 (C≡C), 87.14 (C≡C), 91.51 (C≡C), 120.60 (C-C≡C), 128.06 (Ar, C-H), 131.68 (Ar, C-H), 137.76 (Ar, C-S), 140.02 (Py, C-H_p), 149.90 (Py, C-H_o); one resonance (C-C≡C) not observed, assumed weak/overlapping. IR (ATR): ν (cm⁻¹) 2220 (C≡C). HR-MS ES+: *m/z* 960.1924 ([M+H]⁺ Calc.: 960.1935). (Found: C, 68.61; H, 5.66; N, 1.52. Calc. for C₅₅H₅₃Fe₂NS₂Si₂: C, 68.87; H, 5.56; N, 1.46%).

fc(C(Cl)=C(H)-*p*-C₆H₅)₂ (4-Z)

A mixture of 1,1'-bis(phenylethynyl)ferrocene (0.156 g, 0.40 mmol) and 1.0 M tetra-*n*-butylammonium fluoride in THF (33.5 mL, 33.5 mmol) was stirred at room temperature for 1 h, at which point acetyl chloride (9.2 mL, 129.39 mmol) was added in one portion. CAUTION: addition of acetyl chloride results in a vigorously exothermic reaction. After cooling the solution was diluted into CH₂Cl₂/H₂O (100 mL, 1:1 v/v), whereby the organic fraction was isolated, dried over NaSO₄ and filtered through Celite. The filtrate was concentrated and purified by column chromatography on silica, packing with *n*-hexane and eluting with CH₂Cl₂/*n*-hexane (4:1 v/v). Fractions were carefully selected (using ¹H NMR spectroscopy where necessary), combined and dried *in vacuo* to provide **4-Z** as an orange-red solid (0.116 g, 63%). ¹H NMR (400 MHz, CDCl₃): δ (ppm) 4.39 (pseudo-t, *J*_{αβ} = 1.8 Hz, 4H, Cp-H), 4.67 (pseudo-t, *J*_{αβ} = 1.8 Hz, 4H, Cp-H), 6.82 (s, 2H, C=CH), 7.30 (m, 6H, Ph-H_{m/p}), 7.62 (d, 4H, Ph-H_o). ¹³C{¹H} NMR (100 MHz, CDCl₃): δ (ppm) 68.81 (Cp, C-H), 71.39 (Cp, C-H), 87.41 (Cp, C-C=C), 122.31 (C=C-H), 127.55 (Ph, C-H_p), 128.34 (Ph, C-H_m), 129.31 (Ph, C-H_o), 130.24 (C=C-Cl), 135.45 (Ph, C-

C=C). HR-MS ES+: 458.0291 m/z ($[M]^+$ Calc.: 458.0291). (Found: C, 67.90; H, 4.28. Calc. for $C_{26}H_{20}Cl_2Fe$: C, 68.01; H, 4.39%).

In a analogous experiment it was found that the crude filtrate obtained from dropwise addition of acetyl chloride to an ice-cooled mixture of 1,1'-bis(phenylethynyl)ferrocene and 1.0 M tetra-*n*-butylammonium fluoride in THF provided a more complex 1H NMR spectrum, suggesting the formation of multiple products/isomers. In this case the title product was not readily isolable by recrystallization/column chromatography.

Reaction of **1a** with TBAF/AcCl

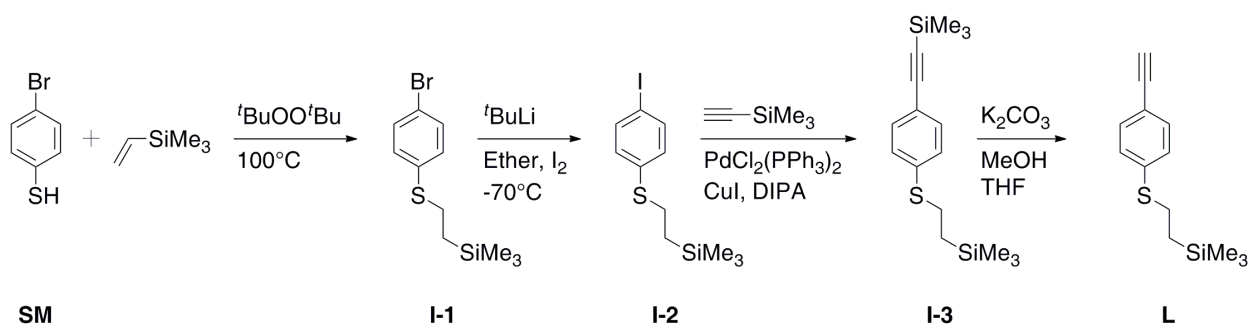
A mixture of **1a** (0.012 g, 0.02 mmol) and 1.0 M tetra-*n*-butylammonium fluoride in THF (1.25 mL, 1.25 mmol) was stirred at room temperature for 1 h, at which point acetyl chloride (0.35 mL, 4.92 mmol) was added in one portion. CAUTION: addition of acetyl chloride results in a vigorously exothermic reaction. After 20 min the solution was diluted into CH_2Cl_2 (15 mL) and H_2O (2.5 mL), whereby the organic fraction was isolated, dried over $NaSO_4$ and filtered through Celite. The filtrate was concentrated and loaded onto a silica column packed with *n*-hexane. Elution with CH_2Cl_2/n -hexane (6:4 v/v) developed an orange band which was collected and dried *in vacuo*. 1H NMR of the orange-red solid showed the presence of multiple products which proved difficult to isolate further by recrystallization/column chromatography. 1H NMR (400 MHz, $CDCl_3$): δ (ppm) 2.38-2.46 (m, C(O)- CH_3), 4.27-4.71 (m, Cp- H), 6.73-7.73 (m, C=C(H)-R and Ar- H). IR (ATR): ν (cm^{-1}) 1703s (C=O), 2208 (C \equiv C). HR-MS ES+: m/z 535.0472 ($[M+H]^+$ Calc. for $C_{30}H_{23}FeO_2S_2$: 535.0489), 552.0714, 571.0236 ($[M+H]^+$ Calc. for $C_{30}H_{24}ClFeO_2S_2$: 571.0255), 588.0508, 606.9993 ($[M+H]^+$ Calc. for $C_{30}H_{25}Cl_2FeO_2S_2$: 607.0022), 624.0263. Please also see Figure S-18 (1H NMR of mixture) and Figure S-19 (annotated mass spectrum of mixture).

Reaction of **fc(C \equiv C-C $_6$ H $_5$) $_2$** with BBr_3 /AcCl

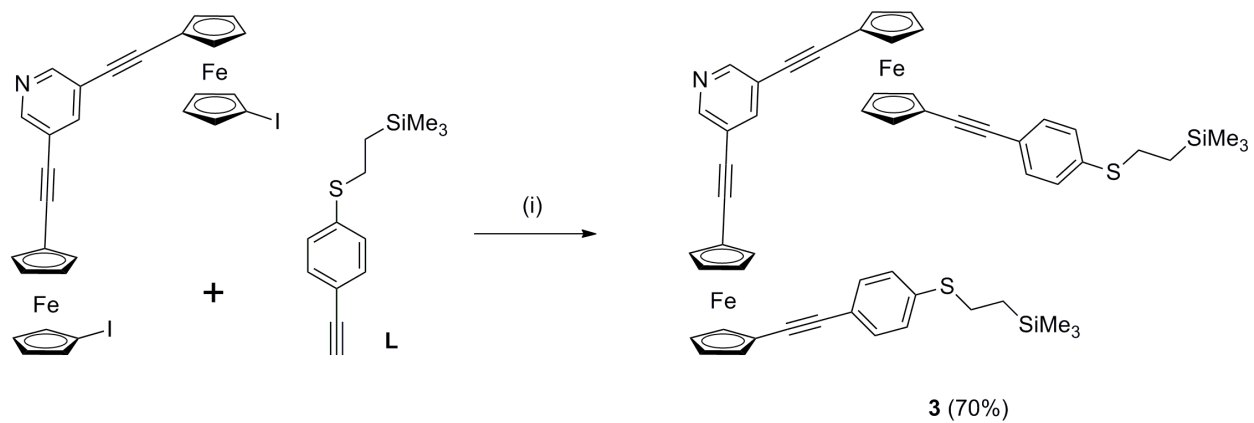
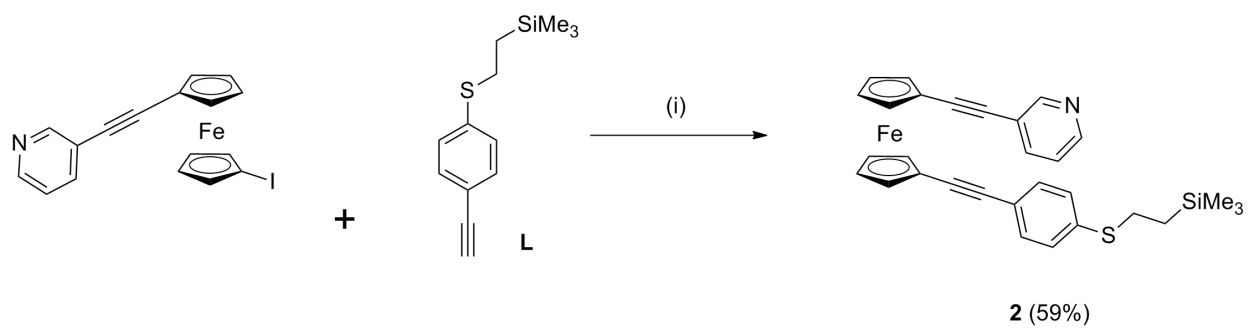
1,1'-Bis(phenylethynyl)ferrocene (0.101 g, 0.26 mmol) and 1.0 M BBr_3 in CH_2Cl_2 (0.29 mL, 0.29 mmol) were added in quick succession to a stirred solution of acetyl chloride (0.125 mL, 1.76 mmol) in toluene (5 mL), whereby the red solution turned black-brown. After 2 h, this mixture was poured onto ice and extracted with CH_2Cl_2 . The organic extracts were dried over $MgSO_4$, filtered through Celite and solvent removed *in vacuo*. 1H NMR of the orange-red solid

showed the presence of multiple products which proved difficult to isolate by recrystallization/column chromatography (silica; CH₂Cl₂/petroleum benzine). ¹H NMR (400 MHz, CDCl₃): δ (ppm) 4.25-4.82 (m, 8H, Cp-H), 6.78-7.78 (m, 12H, C=C(H)-R and Ar-H). IR (ATR): ν (cm⁻¹) 2206 (C≡C). HR-MS ES+: *m/z* 422.0506 ([M+H]⁺ Calc. for C₂₆H₁₉ClFe: 422.0525), 468.0002 ([M+H]⁺ Calc. for C₂₆H₁₉BrFe: 467.9999), 503.9746 ([M+H]⁺ Calc. for C₂₆H₂₀BrClFe: 503.9766), 547.9238 ([M+H]⁺ Calc. for C₂₆H₂₀Br₂Fe: 547.9261). Please also see Figure S-20 (¹H NMR of mixture) and Figure S-21 (annotated mass spectrum of mixture).

REACTION SCHEMES

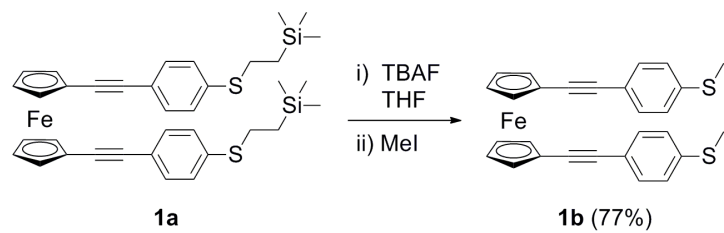


Scheme S-1. Synthesis of 2-(trimethylsilyl)ethyl-4'-ethynylphenyl sulfide (**L**).³



(i) Pd(P^tBu₃)₂, CuI, DIPA, THF

Scheme S-2. Synthesis of 2 and 3.



Scheme S-3. Synthesis of 1b.

$^1\text{H}/^{13}\text{C}\{^1\text{H}\}$ NMR SPECTRA

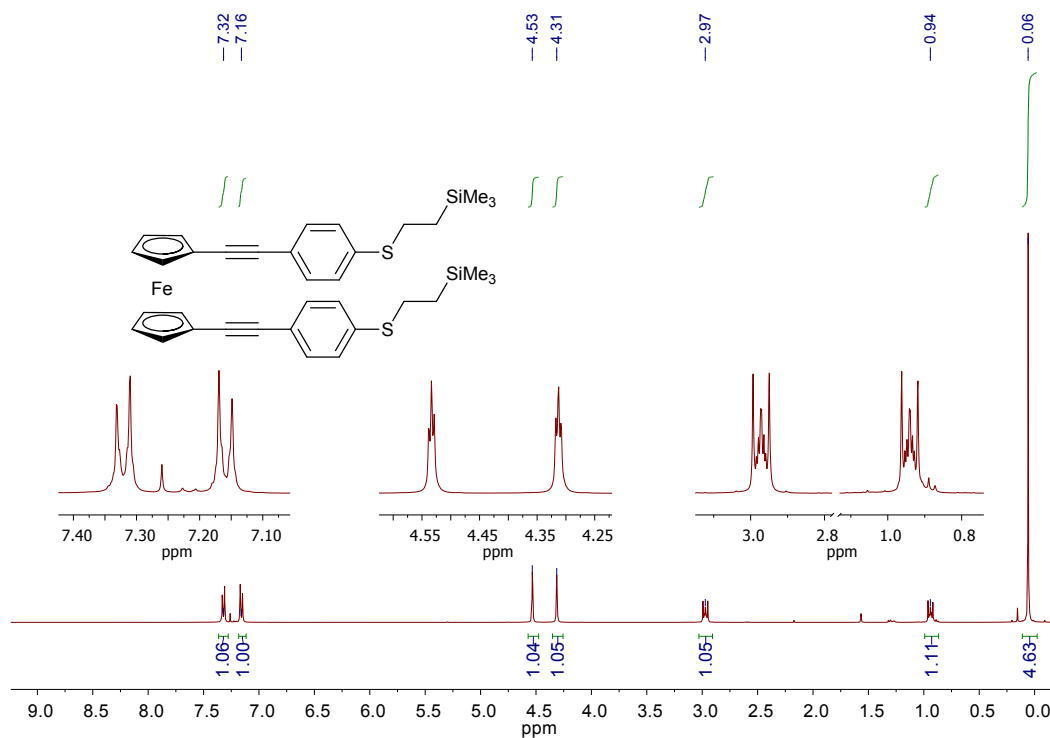


Figure S-1. ¹H NMR spectrum for **1a** in CDCl₃.

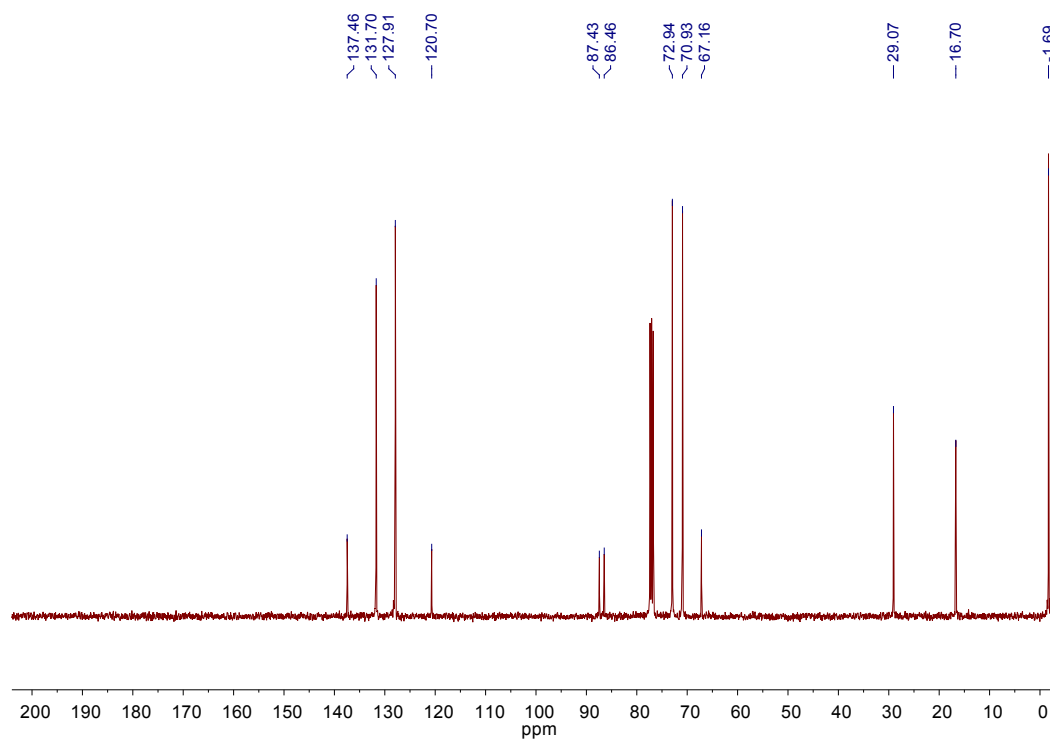


Figure S-2. ¹³C {¹H} NMR spectrum for **1a** in CDCl₃.

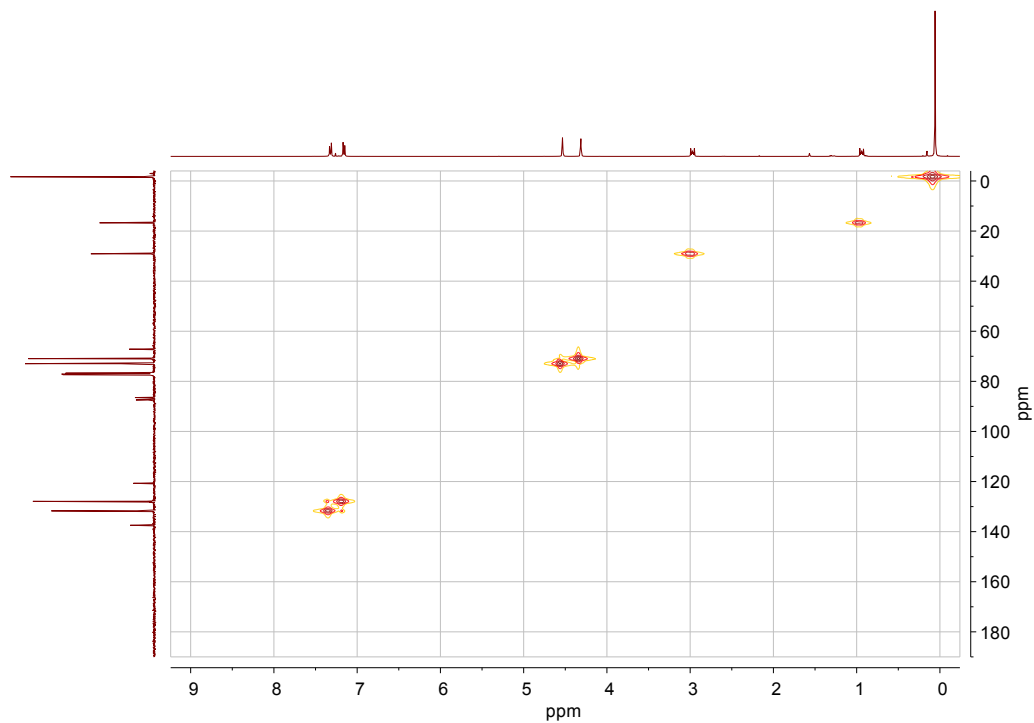


Figure S-3. 2D HMQC (^1H , ^{13}C) NMR spectrum for **1a** in CDCl_3 .

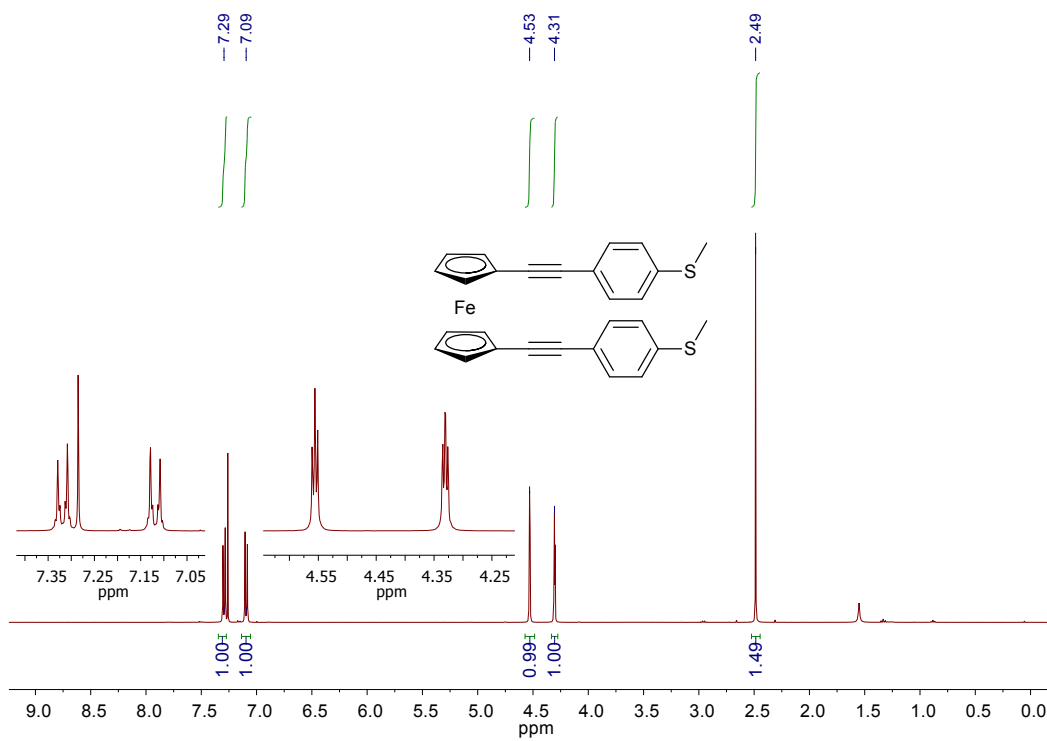


Figure S-4. ^1H NMR spectrum for **1b** in CDCl_3 .

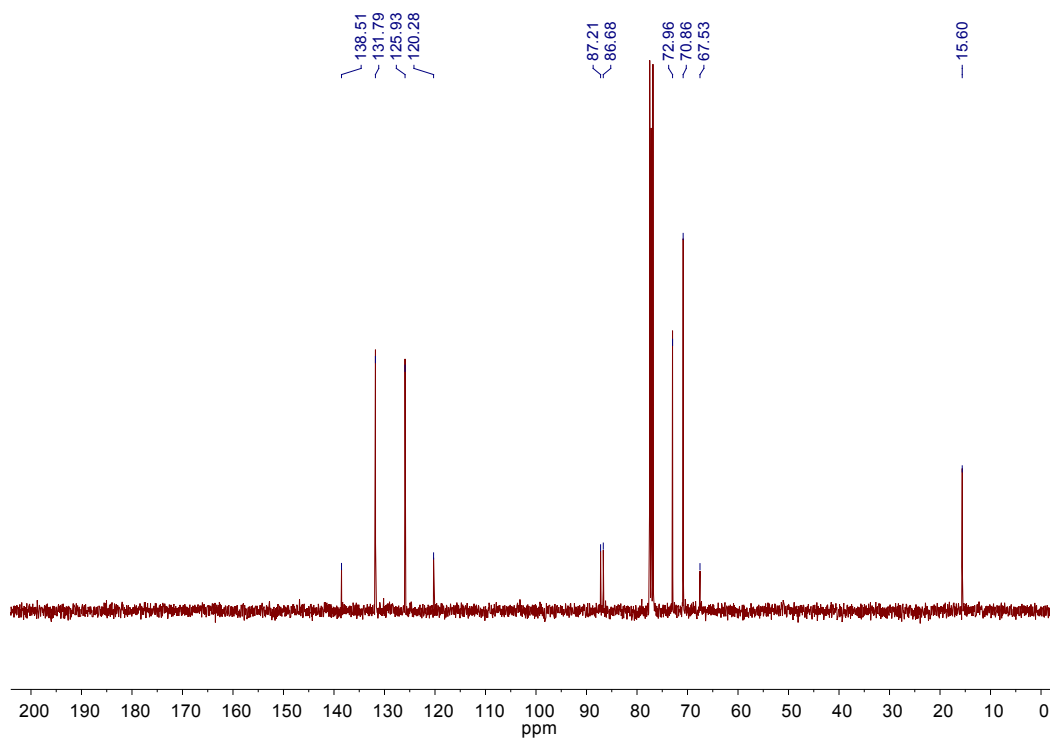


Figure S-5. $^{13}\text{C}\{^1\text{H}\}$ NMR spectrum for **1b** in CDCl_3 .

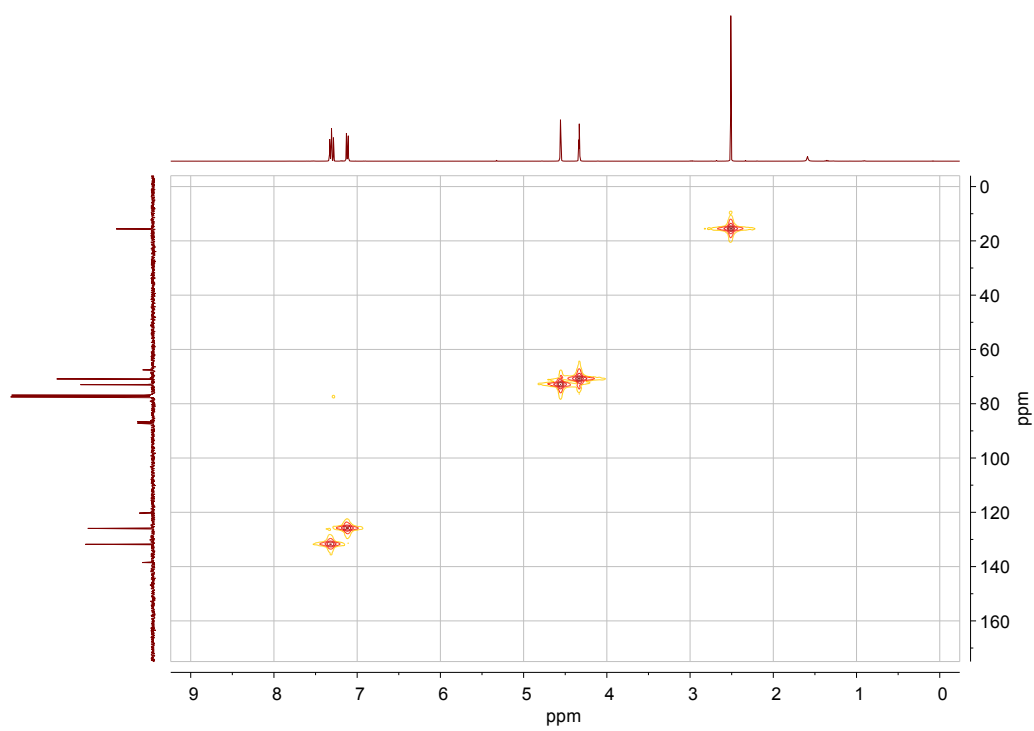


Figure S-6. 2D HMQC (^1H , ^{13}C) NMR spectrum for **1b** in CDCl_3 .

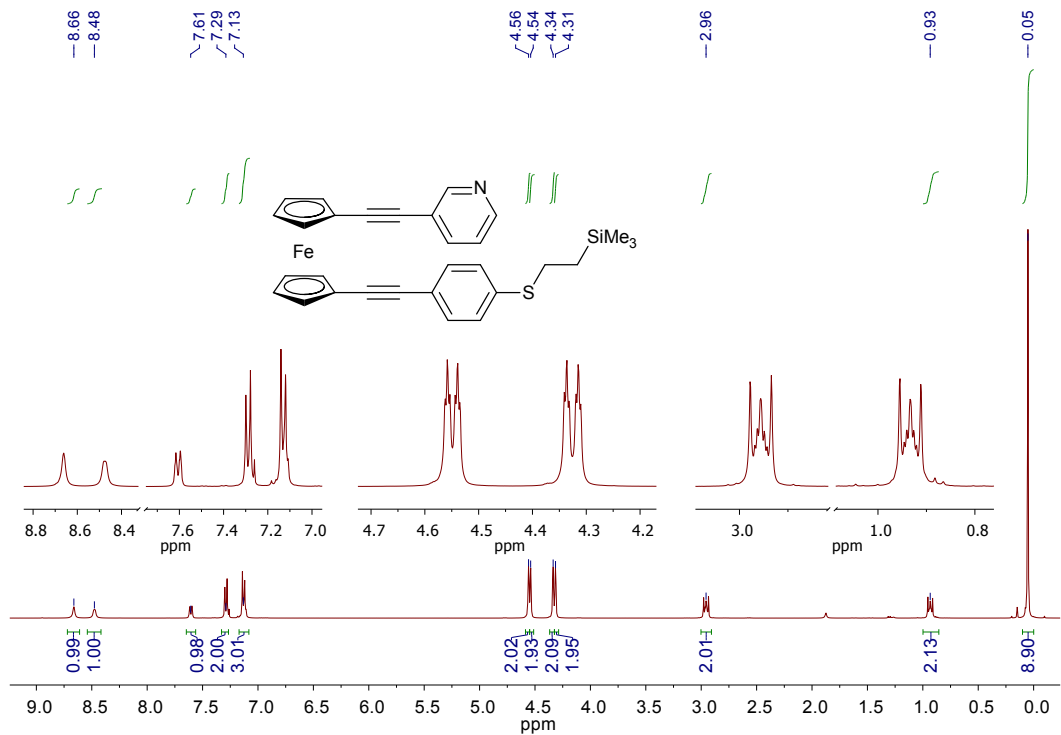


Figure S-7. ¹H NMR spectrum for **2** in CDCl₃.

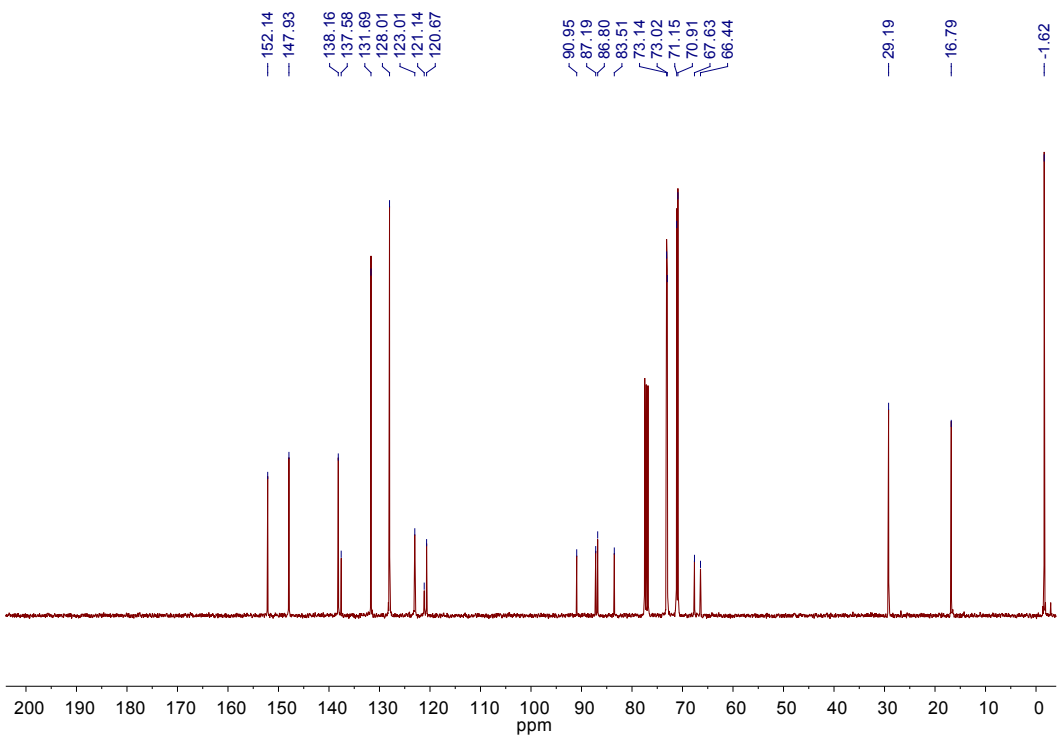


Figure S-8. ¹³C{¹H} NMR spectrum for **2** in CDCl₃.

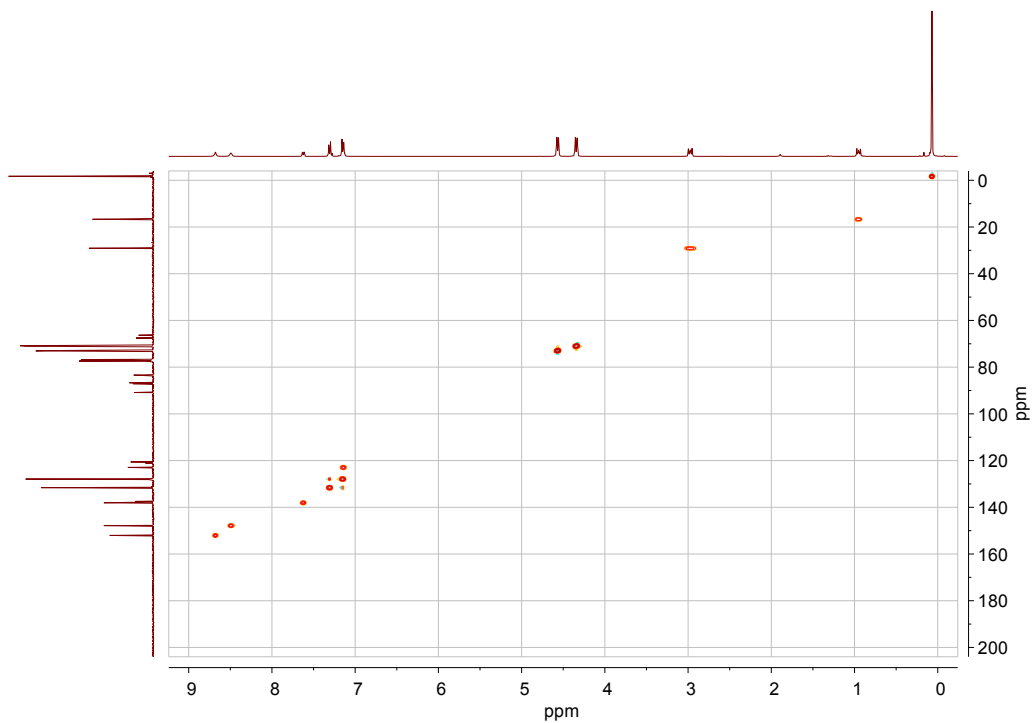


Figure S-9. 2D HSQC (^1H , ^{13}C) NMR spectrum for **2** in CDCl_3 .

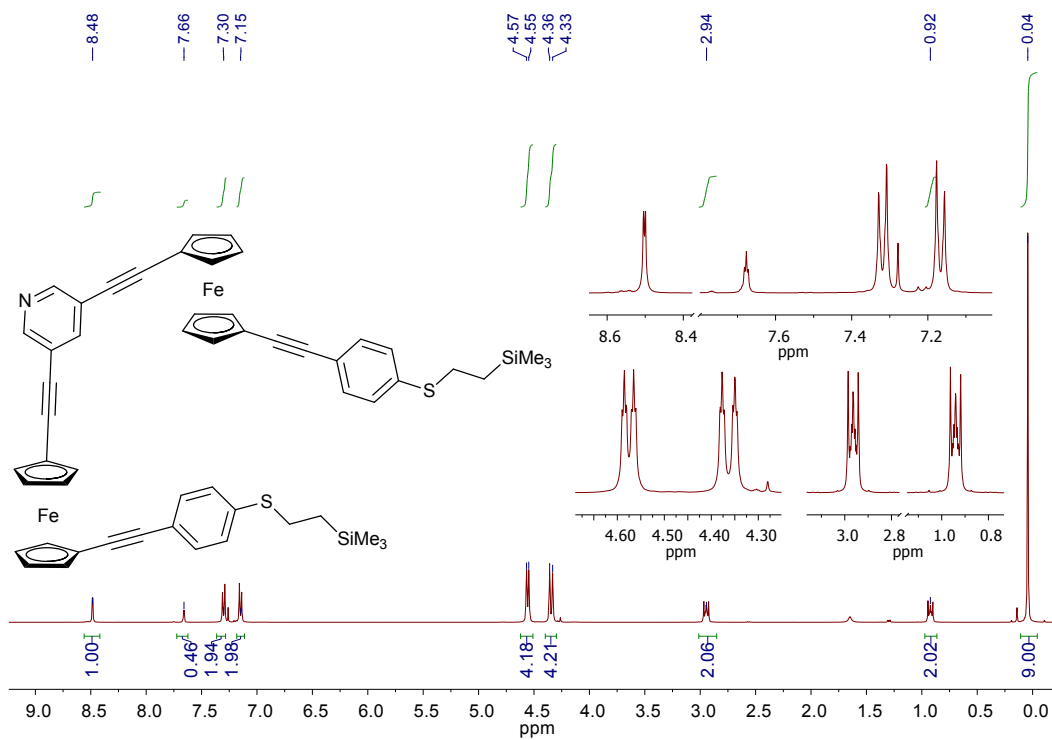


Figure S-10. ^1H NMR spectrum for **3** in CDCl_3

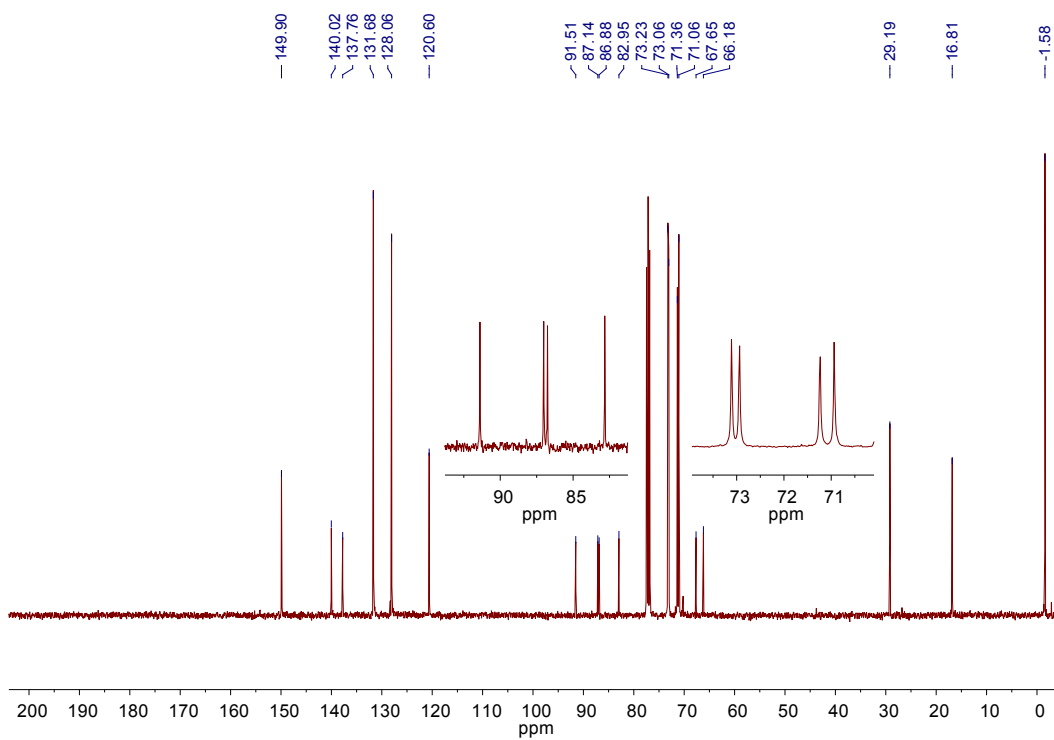


Figure S-11. $^{13}\text{C}\{^1\text{H}\}$ NMR spectrum for **3** in CDCl_3 .

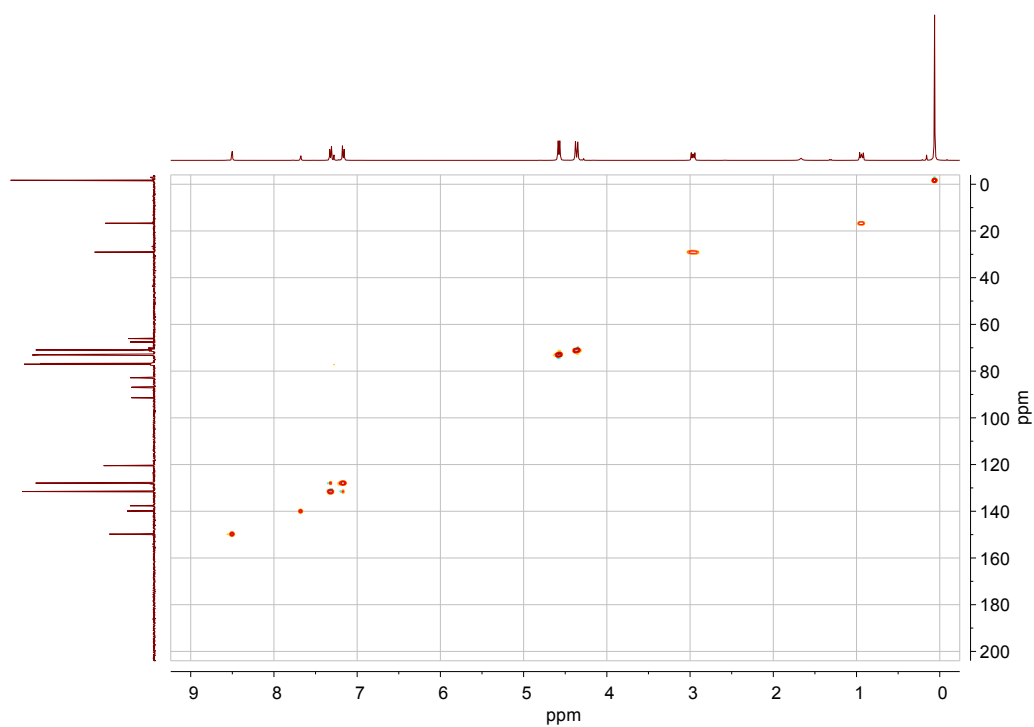


Figure S-12. 2D HSQC (^1H , ^{13}C) NMR spectrum for **3** in CDCl_3 .

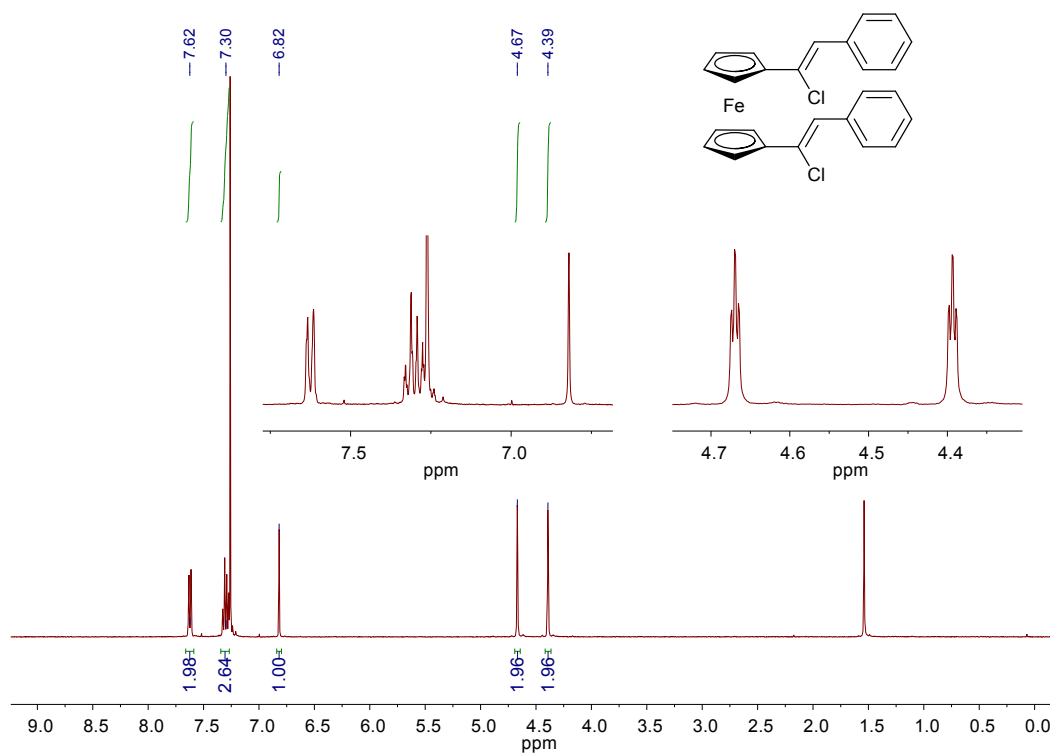


Figure S-13. ^1H NMR spectrum for **4-Z** in CDCl₃.

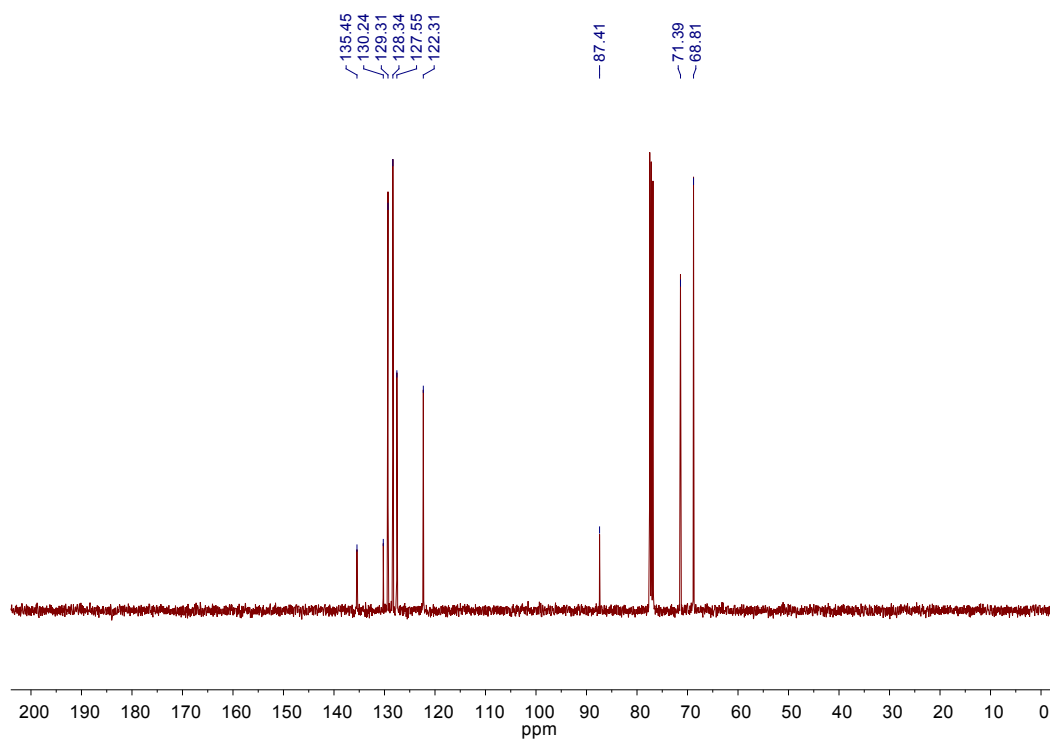


Figure S-14. $^{13}\text{C}\{^1\text{H}\}$ NMR spectrum for **4-Z** in CDCl₃.

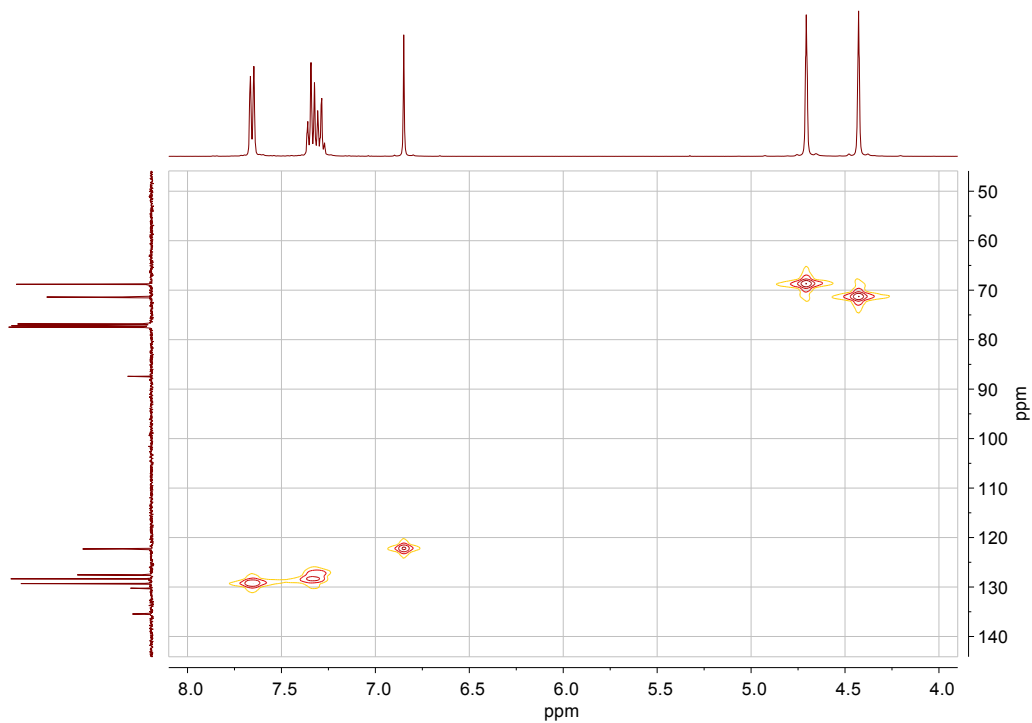


Figure S-15. 2D HMQC (^1H , ^{13}C) NMR spectrum for **4-Z** in CDCl_3 .

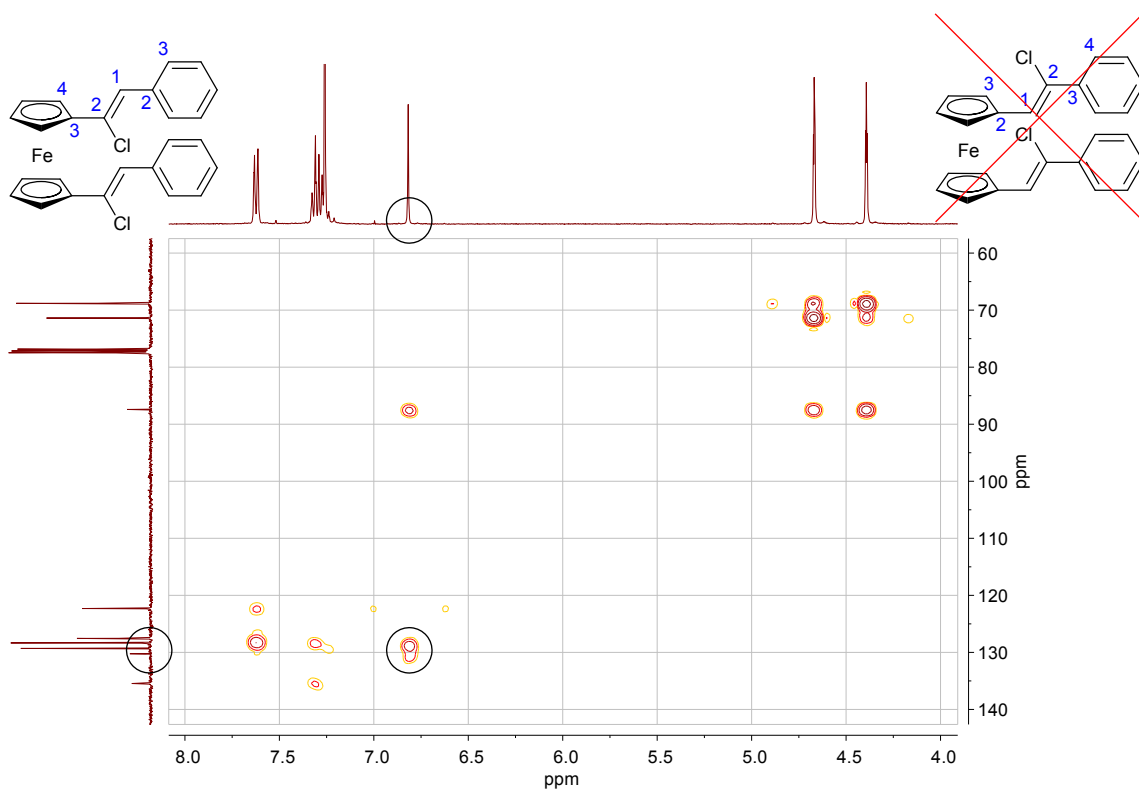


Figure S-16. 2D HMBC (^1H , ^{13}C) NMR spectrum for **4-Z** in CDCl_3 . Cross peaks between vinyl proton and phenyl carbon resonances (black circles) indicate coupling through 2-4 bonds.

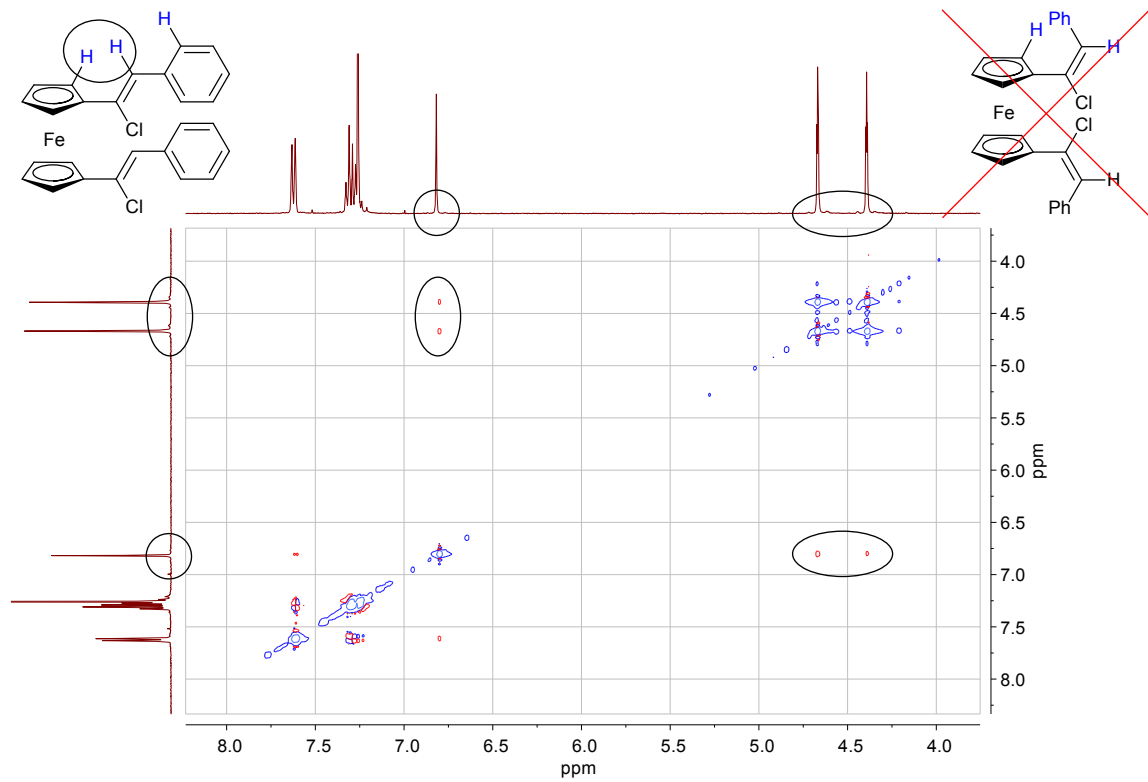


Figure S-17. 2D ROESY (^1H , ^1H) NMR spectrum for **4-Z** in CDCl_3 . Cross peaks between vinyl and cyclopentadienyl proton resonances (black circles) indicate closeness in space.

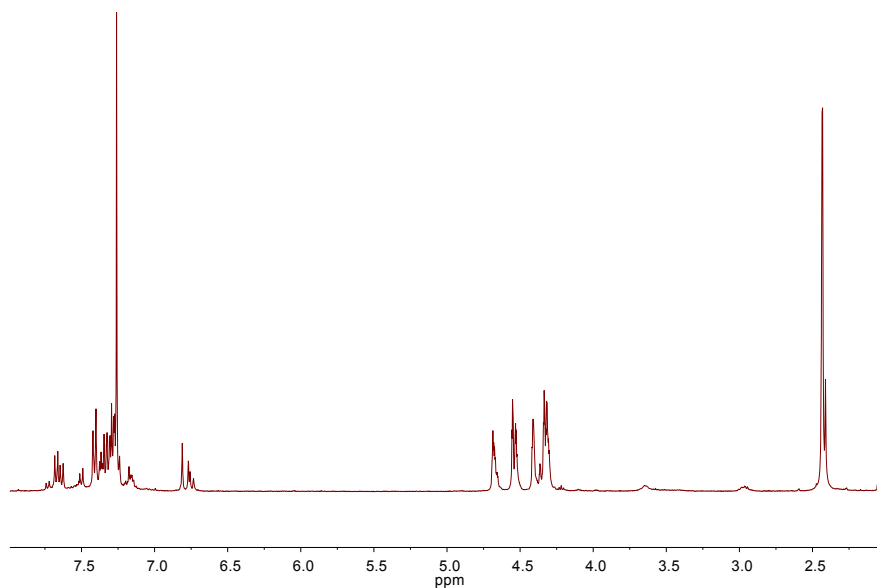


Figure S-18. ^1H NMR spectrum of the crude mixture following reaction of **1a** with TBAF/AcCl.

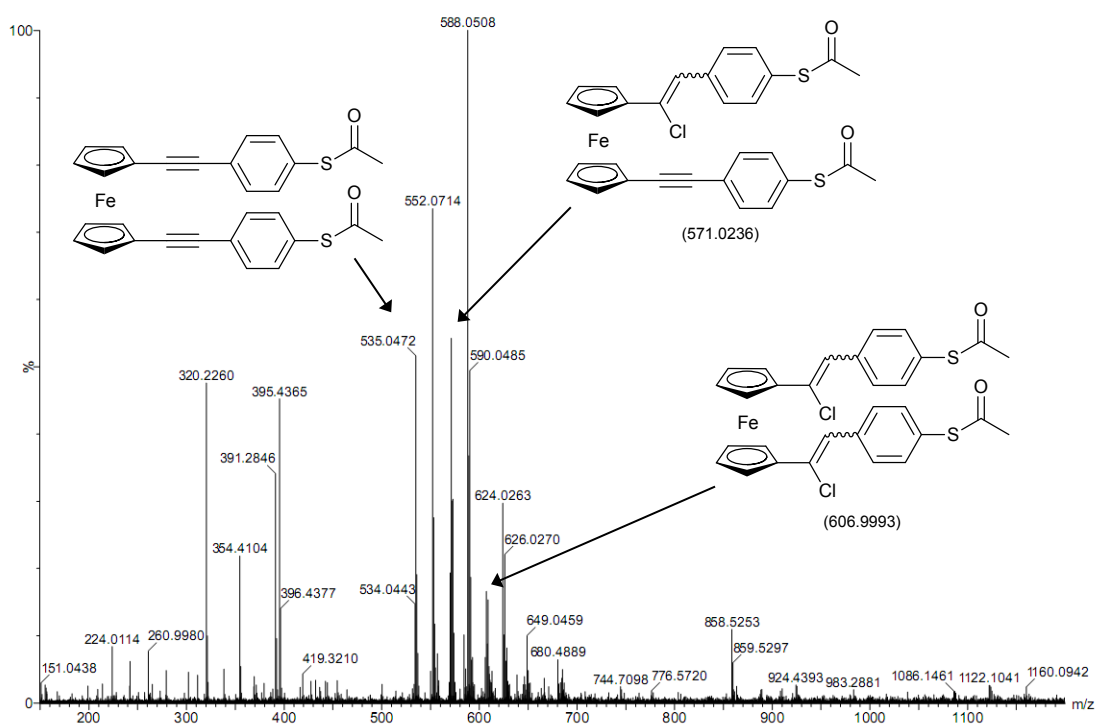


Figure S-19. Mass spectrum of the crude mixture following reaction of **1a** with TBAF/AcCl (a series of unidentified ions/products are observed at 552.0714, 588.0508 and 624.0263 m/z). Note, Markovnikov product structures added for clarity only. Regio- and stereochemical assignment of components in mixtures was impracticable due to overlapping resonances in their NMR spectra.

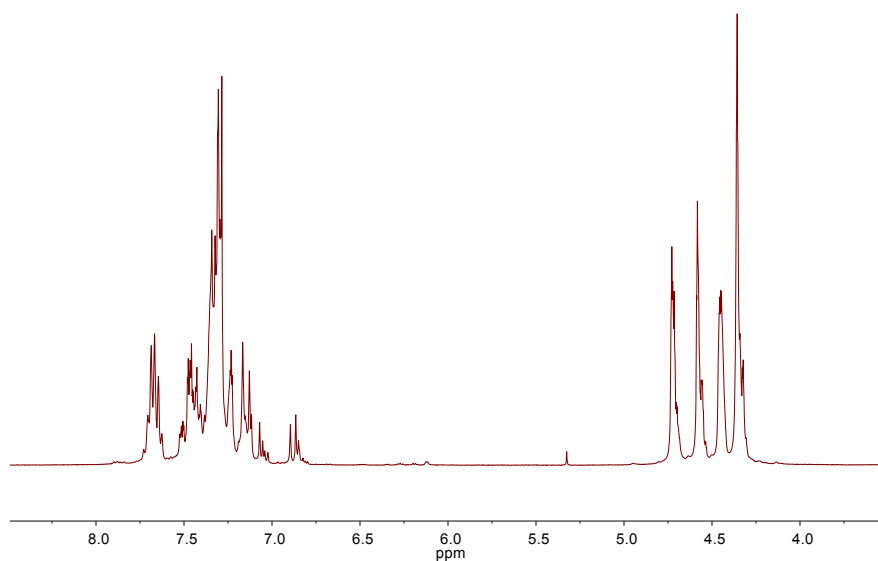


Figure S-20. ^1H NMR spectrum of the crude mixture following reaction of $\text{fc}(\text{C}\equiv\text{C}-\text{C}_6\text{H}_5)_2$ with BBr_3/AcCl .

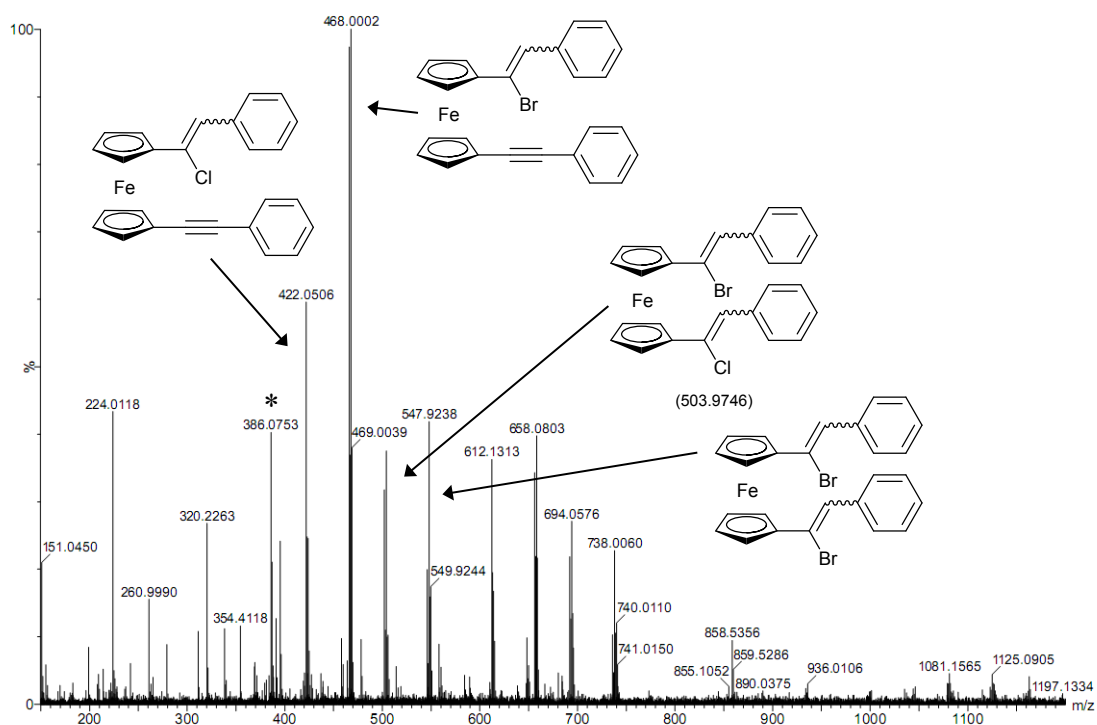


Figure S-21. Mass spectrum of the crude mixture following reaction of $\text{fc}(\text{C}\equiv\text{C}-\text{C}_6\text{H}_5)_2$ with BBr_3/AcCl (starred peak corresponds to starting material). Note, Markovnikov product structures added for clarity only. Regio- and stereochemical assignment of components in mixtures was impracticable due to overlapping resonances in their NMR spectra.

ELECTROCHEMISTRY

The redox properties of **1-4** were investigated via solution/surface cyclic voltammetry (CV), and where relevant differential pulse voltammetry (DPV), in CH₂Cl₂/0.1 M ⁿBu₄NPF₆, CH₂Cl₂/~0.02 M Na[B(C₆H₃(CF₃)₂)₄] (a saturated solution) or CH₃CN/0.1 M ⁿBu₄NPF₆. Relevant data are summarized in Table S-1.

Table S-1. Electrochemical data for 1,1'-substituted ferrocene complexes.^a

compound	E_{pa} (V)	E_{pc} (V)	ΔE (mV)	i_p^a/i_p^c	$E_{1/2}^b$ (V)
fc(C≡C- <i>p</i> -C ₆ H ₄ -S-CH ₂ CH ₂ -SiMe ₃) ₂ (1a)	0.25	0.20	53	0.96	0.23
fc(C≡C- <i>p</i> -C ₆ H ₄ -S-Me) ₂ (1b)	0.25	0.20	59	0.97	0.22
fc(C≡C- <i>p</i> -C ₆ H ₄ -S-Me) ₂ (1b-Au) ^c	0.34	0.28	58 ^d	0.87 ^d	0.31
fc(C≡C- <i>p</i> -C ₆ H ₄ -S ⁻) ₂ (1c-Au) ^c	0.28	0.27	9	1.06	0.28
fc(C≡C- <i>m</i> -Py)(C≡C- <i>p</i> -C ₆ H ₄ -S-CH ₂ CH ₂ -SiMe ₃) (2)	0.33	0.24	81	1.01	0.29
(μ -3,5-Py)(C≡C-[fc]-C≡C- <i>p</i> -C ₆ H ₄ -S-CH ₂ CH ₂ -SiMe ₃) (3)					
- CH ₂ Cl ₂ /0.1 M ⁿ Bu ₄ NPF ₆	0.31	0.24	75	1.03	0.28
- CH ₂ Cl ₂ /~0.02 M Na[B(C ₆ H ₃ (CF ₃) ₂) ₄] ^e	0.44	0.38	60	1.04	0.41
fc(C(H)=C(Cl)- <i>p</i> -C ₆ H ₅) ₂ (4)	0.27	0.19	80	0.92	0.23

^a Solution voltammetry conditions (unless otherwise stated): scan rate 0.1 Vs⁻¹; reaction medium, CH₂Cl₂/0.1 M ⁿBu₄NPF₆; working electrode, glassy carbon; reference and counter electrodes, Pt. All potentials assigned to the Fe²⁺/Fe³⁺ couple, measured against an internal [FeCp*₂]^{+/}[FeCp*₂] reference, reported relative to [FeCp₂]^{+/}[FeCp₂] (0.495 V vs. [FeCp*₂]^{+/}[FeCp*₂]) and corrected for iR_s . ^b $E_{1/2} = 1/2(E_{pa} + E_{pc})$. ^c Surface voltammetry conditions: scan rate 0.1 Vs⁻¹; reaction medium, CH₃CN/0.1 M ⁿBu₄NPF₆; working electrode, surface-modified gold bead; reference and counter electrodes, Pt. ^d Deviations from ideal reversible behaviour are attributed to difficulties in defining the baseline for the reduction process. ^e Shoulder and peak (Fig. S-22) coalesce upon addition of [FeCp*₂]^{+/}[FeCp*₂], electrochemical data obtained from the mixed solution.

Further to discussions in the main text, all *solution* species demonstrated close to reversible behavior ($i_p^a/i_p^c \approx 1$, $i_p \propto V_s^{1/2}$, and in the majority of cases $\Delta E \sim 59$ mV). Redox features were assigned to the Fe²⁺/Fe³⁺ couple, with $E_{1/2}$ values comparable to those observed for

(arylethynyl)ferrocenes reported elsewhere.^{4,8} Equilibrium potentials follow anticipated trends, with $E_{1/2}(\mathbf{1a}/\mathbf{1b}) > E_{1/2}(\mathbf{2}/\mathbf{3})$, indicating that pyridyl moieties are more electron withdrawing than their arylthioether counterparts. For bimetallic complex **3** (comprising a reasonably bulky terminal substituent, $-\text{CH}_2\text{CH}_2\text{SiMe}_3$), changing the reaction medium from $\text{CH}_2\text{Cl}_2/0.1 \text{ M } ^n\text{Bu}_4\text{NPF}_6$ to $\text{CH}_2\text{Cl}_2/\sim 0.02 \text{ M Na}[\text{B}(\text{C}_6\text{H}_3(\text{CF}_3)_2)_4]$ ⁹ favours formation of the mixed valence species in line with our previous discussions.⁴ This is evidenced by a splitting of the redox feature (Fig. S-22), where the two overlapping waves are attributed to $[\text{Fe}_1^{2+}\text{Fe}_2^{2+}]^0/[\text{Fe}_1^{3+}\text{Fe}_2^{2+}]^+$ (E_1) and $[\text{Fe}_1^{3+}\text{Fe}_2^{2+}]^+ / [\text{Fe}_1^{3+}\text{Fe}_2^{3+}]^{2+}$ (E_2) redox processes.

Interestingly, we observed an additional shoulder feature in the differential pulse voltammogram (as indicated by the arrow, Fig. S-22, bottom). This is not apparent in the cyclic voltammogram of the same system, acquired a few scans previously (Fig. S-22, top). Whilst the physical origin of this spectral characteristic is not yet clear, we note that a similar, albeit less-pronounced, peak was also present in the DPV of a S'Bu-terminated analogue.⁴

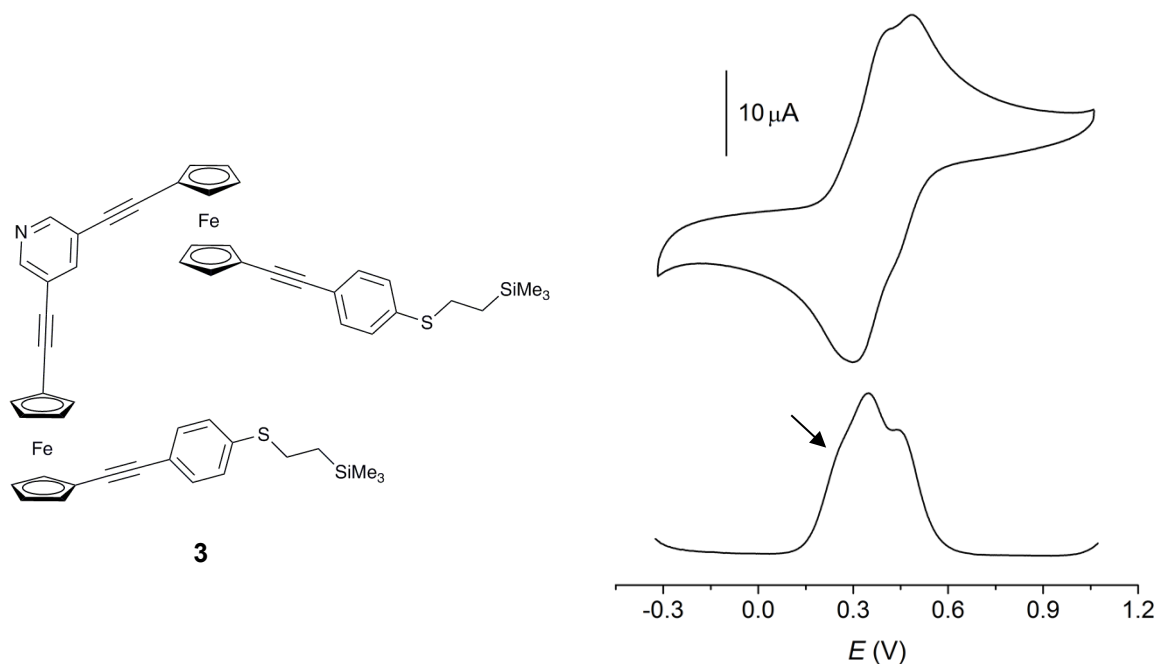


Figure S-22. Solution cyclic (right top, corrected for iR_s) and differential pulse (right bottom) voltammograms for **3** (left), recorded in $\text{CH}_2\text{Cl}_2/\text{Na}[\text{B}(\text{C}_6\text{H}_3(\text{CF}_3)_2)_4]$ ($\sim 0.02 \text{ M}$). Potentials are reported vs. $[\text{FeCp}_2]^+ / [\text{FeCp}_2]$.

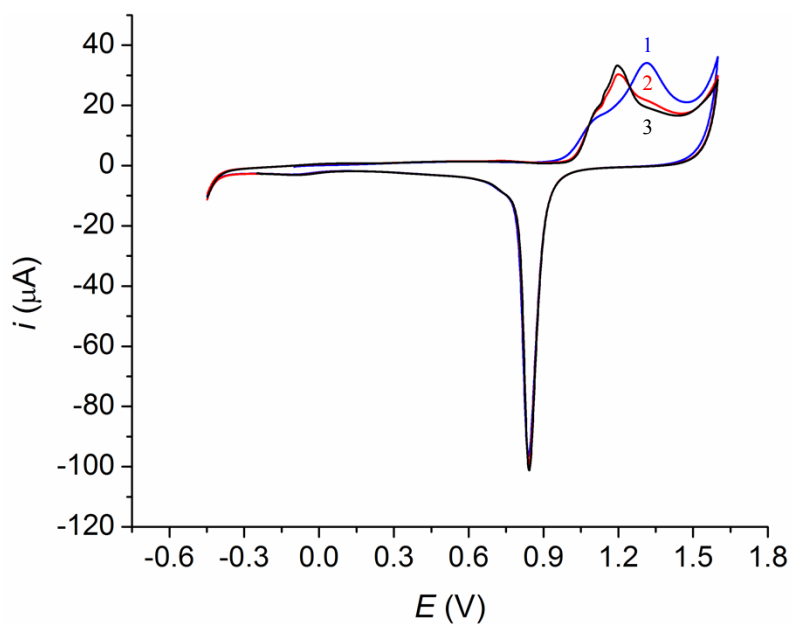


Figure S-23. Cyclic voltammetry of **1c-Au** in $\text{H}_2\text{O}/0.1 \text{ M HClO}_4$ with Pt wire counter and Ag/AgCl reference electrodes (scan rate 0.1 Vs^{-1}). Features related to gold oxidation/reduction are apparent, and interfere with the redox chemistry of the layer.

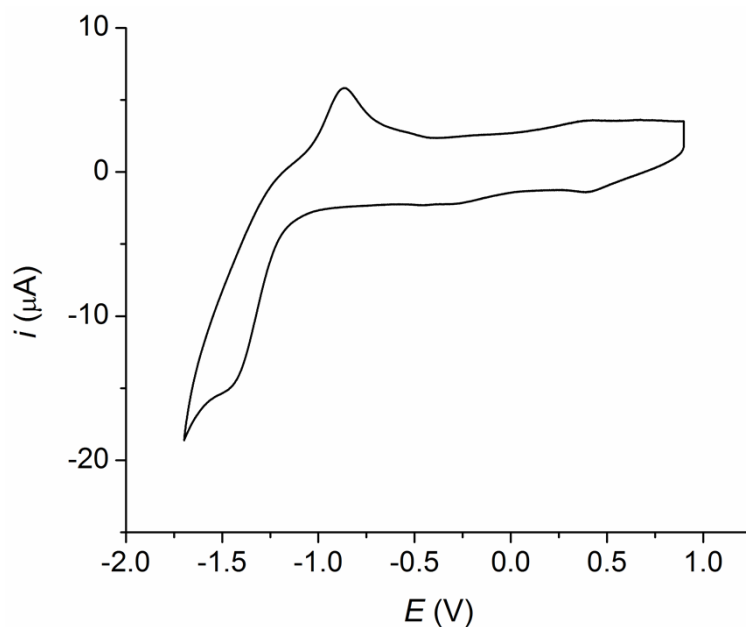


Figure S-24. A cyclic voltammogram conducted in $\text{CH}_3\text{CN}/0.1 \text{ M } t\text{Bu}_4\text{NPF}_6$ using an Au bead working electrode (freshly annealed in a H_2 flame), Pt counter and reference electrodes (scan rate 0.5 Vs^{-1}).

X-RAY CRYSTALLOGRAPHY

The X-ray crystal structure of **1a**

The structure of **1a** was found to contain two crystallographically independent molecules (**A** and **B**) in the asymmetric unit. The S(1)-bound $\text{CH}_2\text{CH}_2\text{SiMe}_3$ unit in molecule **B** was found to be severely disordered. Three orientations were identified of *ca.* 53, 33 and 14% occupancy, their geometries were optimised, the thermal parameters of adjacent atoms were restrained to be similar, and only the non-hydrogen atoms of the major occupancy orientation were refined anisotropically (those of the minor occupancy orientation were refined isotropically).

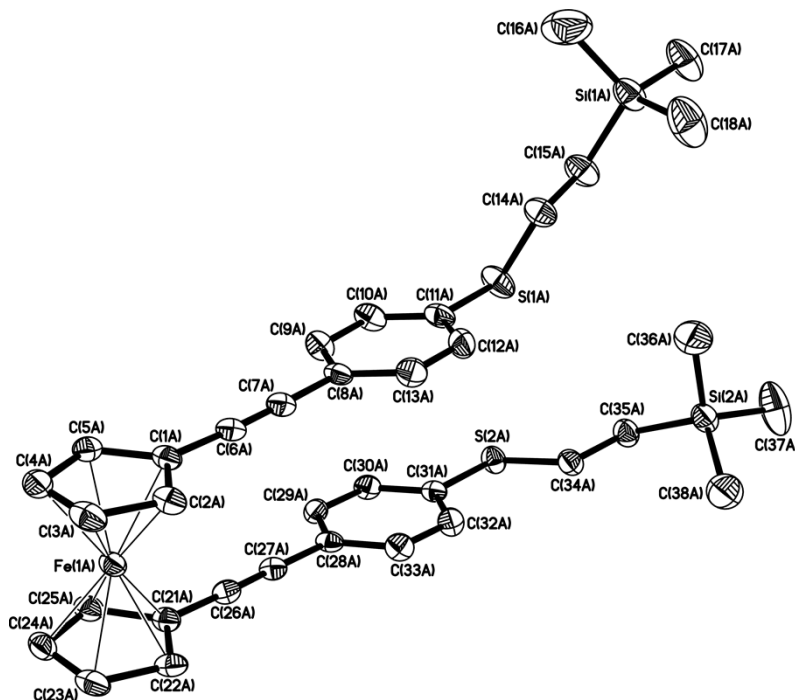


Figure S-25. The structure of one (**1a-A**) of the two independent molecules present in the crystal of **1a** (50% probability ellipsoids).

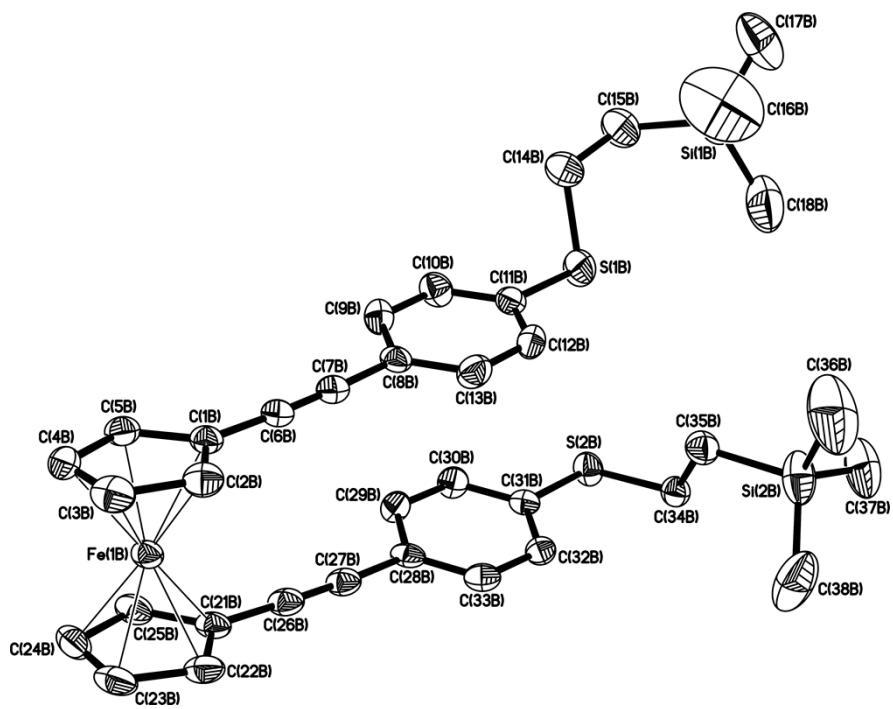


Figure S-26. The structure of one (**1a-B**) of the two independent molecules present in the crystal of **1a** (50% probability ellipsoids).

REFERENCES

1. D. B. G. Williams and M. Lawton, *J. Org. Chem.*, 2010, **75**, 8351.
2. M. S. Inkpen, S. Du, M. Driver, T. Albrecht and N. J. Long, *Dalton Trans.*, 2013, **42**, 2813.
3. C. J. Yu, Y. Chong, J. F. Kayyem and M. Gozin, *J. Org. Chem.*, 1999, **64**, 2070.
4. M. S. Inkpen, T. Albrecht and N. J. Long, *Organometallics*, 2013, **32**, 6053.
5. M. S. Inkpen, A. J. P. White, T. Albrecht and N. J. Long, *Chem. Commun.*, 2013.
6. G. R. Fulmer, A. J. M. Miller, N. H. Sherden, H. E. Gottlieb, A. Nudelman, B. M. Stoltz, J. E. Bercaw and K. I. Goldberg, *Organometallics*, 2010, **29**, 2176.
7. S. Creager, C. J. Yu, C. Bamdad, S. O'Connor, T. MacLean, E. Lam, Y. Chong, G. T. Olsen, J. Luo, M. Gozin and J. F. Kayyem, *J. Am. Chem. Soc.*, 1999, **121**, 1059.
8. (a) C. Engtrakul and L. R. Sita, *Organometallics*, 2008, **27**, 927; (b) J. Ma, M. Vollmann, H. Menzel, S. Pohle and H. Butenschön, *J. Inorg. Organomet. Polym. Mater.*, 2008, **18**, 41; (c) I. Baumgardt and H. Butenschön, *Eur. J. Inorg. Chem.*, 2010, **2010**, 1076; (d) C. Engtrakul and L. R. Sita, *Nano Lett.*, 2001, **1**, 541.
9. (a) F. Barrière, N. Camire, W. E. Geiger, U. T. Mueller-Westerhoff and R. Sanders, *J. Am. Chem. Soc.*, 2002, **124**, 7262; (b) F. Barrière and W. E. Geiger, *J. Am. Chem. Soc.*, 2006, **128**, 3980.